Journal of the Korean Institute of Industrial Engineers
Vol. 52, No. 1, pp. 1-12, February 2026.
ISSN 1225-0988 | EISSN 2234-6457
https://doi.org/10.7232/JKIIE.2026.52.1.001

전기자동차 배터리 상태 예측을 위한 물리 기반 특징 추출 및 전이 프레임워크

Raghda Mansour Kamel Noureldin · 이현수†

국립 금오공과대학교 산업공학과

Effective Physics-guided Feature Transfer Framework for Electric Vehicle Battery Status Prediction

Raghda Mansour Kamel Noureldin · Hyunsoo Lee

Department of Industrial Engineering, Kumoh National Institute of Technology

Physics-based hybrid machine learning models are gaining popularity due to their ability to capture both known physics and unknown dynamics introduced by sensory data. However, such models are often large and computationally intensive compared to purely data-driven models. To address this challenge, this study proposes a physics-guided feature transfer (PgFT) framework that selectively extract the physical and meaningful features from a pretrained hybrid physics-data model to a functional learner model. The functional learner is a light-sized predictor lessening learning burdens with guarantying high accuracy. The proposed framework is modeled for predicting the battery performance of an electric vehicle (EV) under real-world operation scenarios. Despite the accounted dynamic noise and significant nonlinearities in each scenario, the functional learner model－trained using the PgFT strategy－successfully learns the key physical behaviors and adapts an EV dynamically.

Keywords: Physics-based Hybrid Deep Learning, Physics-guided Feature Transfer, Functional Learner, Electric Vehicle Battery Dynamics

1. Introduction

The rapid adoption of electric vehicles (EVs) has increased the demand for accurate and efficient battery management systems (BMS) capable of estimating internal states such as state of charge (SoC) and heat generation. These internal states are critical to ensure battery safety, longevity, and performance. Improper management of these key states may lead to severe consequences, including thermal runaway－an extreme failure mode that poses serious risks to both the vehicle and its occupants. However, in reality, EVs operate in diverse and time-varying conditions－cycling through driving, charging, and parking phases－each of which imposes distinct thermal, mechanical, and electrical stresses on the battery. Transitions among these phases, particularly from high load driving to immediate charging or expanded parking, often lead to complex and strongly coupled electro-thermal dynamics. Despite recent advances having focused on real-time battery diagnostics, most existing modeling approaches focus on each operation phase independently. As a result, they often fail to account for the dynamics occurring during transitions, which are critical for capturing battery behavior more accurately. This limitation becomes particularly noticeable when considering extreme environmental conditions or rapid switching between operation

This work was supported by the IITP(Institute of Information & Communications Technology Planning & Evaluation)-ITRC(Information Technology Research Center) grant funded by the Korea government(Ministry of Science and ICT)(IITP-2025-RS-2024-00438430)
† 연락저자 : 이현수 교수, 39177 경상북도 구미시 대학로 61 금오공과대학교 산업공학부, Tel : 054-478-7661, Fax : 054-478-7679, E-mail : hsl@kumoh.ac.kr
2025년 7월 29일 접수; 2025년 8월 25일 수정본 접수; 2025년 10월 22일 게재 확정.

modes, where thermal buildup or sudden SoC changes can significantly affect EVs' performance. To address these challenges, this study considers real-life operation phases of an EV under different environmental conditions. Based on each scenario, a hybrid physics-based model incorporating noise terms is developed for accurately predicting SoC and heat generation capturing real-life dynamics.

Recent advances in physics-based neural networks (PBNNs) and data-driven models have shown promise in capturing nonlinear battery behaviors. While PBNNs integrate physical dynamics into the learning process to enhance generalizability, they are often computationally intensive, making them impractical for real-time applications or large-scale deployment. On the other hand, purely data-driven models offer fast inference but frequently struggle to generalize across unseen operating conditions or capture underlying physical dependencies.

To address these limitations, this study proposes a novel hybrid deep learning framework that combines the strengths of physics-based and data-based modeling while reducing deployment complexity. Specifically, we develop a multi-stream hybrid model comprising one PBNN-based stream for SoC, one PBNN-based stream for heat generation, and one data-driven stream for the both EV battery states. The proposed framework is trained using various operation and physics data of EVs that span diverse operational conditions and environmental extremes alongside physics-based energy constraints. From this comprehensive hybrid model, we distill physical knowledge into a lightweight, single-stream, data-driven, functional learner model using a novel physics-guided feature transfer (PgFT) framework.

The remainder of this study is organized as follows. Section 2 presents a comprehensive review of related literature and relevant background information. Section 3 describes real-life EV operations and the associated battery physics. Section 4 introduces the proposed framework and provides detailed methodologies for predicting SoC and heat generation in an EV battery system. Finally, the effectiveness of the proposed framework is demonstrated through comparative analyses with other proposed feature sharing models.

2. Background and Literature Review

According to Kim *et al.* (2019), the battery is the most critical component of an EV system. From a sustainability perspective, the manufacturing of EV battery packs requires the extraction of significant amounts of rare and valuable materials such as lithium and cobalt. Therefore, extending battery lifespan and reducing degradation are essential goals for sustainable EV development. Among various EV battery performance indices, this study focuses on both key internal states: SoC and heat generation.

Numerous studies have been conducted to predict and to manage these internal states. Wu *et al.* (2024) approximated battery dynamics using the Bernardi equation, which focused on battery current variation over the sampling time. In their work, heat generation was attributed primarily to Joule (ohmic) heating and reversible entropy change, the two dominant components influencing thermal behavior in battery systems. Ceraolo *et al.* (2024) refined a Bernardi equation-based model by distinguishing between different resistive loss mechanisms－specifically separating static and dynamic resistances －rather than using a single aggregated Joule heat term. Chen *et al.* (2024) contributed to the Bernardi equation by expressing current as a function of motor power demand, internal resistance, and open-circuit voltage. This formulation provides a deeper and more realistic view of heat generation under dynamic driving conditions, enhancing the classical model's applicability. Kumar *et al.* (2023) offered a broader perspective in their comprehensive review of battery modeling approaches. They discussed energy balance-based thermal models, which account for both heat generation and heat dissipation processes. In terms of SoC estimation, they discussed several widely used methods, including the ampere-hour integration method, equivalent circuit models (ECMs), and the open-circuit voltage (OCV) lookup table approach.

<Table 1> summarizes additional key studies for estimating battery states, with particular focuses on SoC and heat generation, as these are the key indicators explored in this study.

As mentioned earlier, a number of studies have developed physics-based models to estimate both SoC and heat generation. In general, physics-based deep learning model has demonstrated success in capturing the nonlinear behaviors inherent in physical systems. The integration of physics into deep learning has been performed in several forms in recent research studies－ in which some approaches embed physical laws directly into the neural network structure, while others incorporate them into the loss (energy) function. Guo *et al.* (2022) incorporated physics at the first hidden layer of their neural network model. While traditional deep learning models connect the input layer to the first hidden layer using standard parameterized transformations, their approach replaces this connection with a physics-driven formulation. Similarly, Seyed-Ahmadi *et al.* (2022) proposed a physics-inspired neural network based on the idea that physical influence propagates through neighbor interactions, assuming that the total effect is the sum of individual contributions－reflecting the idea that physical interactions are governed by the same law for every neighbor. Apostolakis and Ampountolas (2024) extended this line of work by incorporating physics into both the neural network architecture and the loss function, representing a more stringent

Table 1. Existing SoC and Heat Estimation Models

Study	Application	Estimation framework
Chianese *et al.* (2025)	SoC model	Feed-Forward Neural Network (FFNN), Long Short-Term Memory (LSTM), Convolutional Neural Network (CNN) trained on simulated data from a validated electro- thermal ECM model.
Li *et al.* (2022)	SoC and Capacity	Hybrid machine learning framework: Gaussian Process Regression (GPR) for SoC, and CNN for capacity, both enhanced sensor data (strain and temperature).
Yalçın *et al.* (2022)	Heat generation rate (HGR)	CNN and Artificial Bee Colony (ABC) optimization.
Wang *et al.* (2024)	HGR	Neural Network using Principal Component Analysis (PCA), Bayesian Optimization (BO), and Adam Optimizer.
Pang *et al.* (2023)	HGR	Physics-Informed Neural Network (PINN) combining Single Particle Thermodynamics Model (SPMT) with Bayesian-optimized Bidirectional Long Short-Term Memory (BiLSTM).
Maheshwari and Nageswari (2022)	SoC model	Two-Resistor-Capacitor (RC) Equivalent Circuit Model (ECM) and Extended Kalman Filter (EKF) with noise covariance matrices optimized by Sunflower Optimization Algorithm (SFO).
Zahid *et al.* (2018)	SoC model	Subtractive Clustering Adaptive Neuro-Fuzzy Inference System (SC-ANFIS).
Mesbahi *et al.* (2021)	SoC and heat estimation	Coupled distributed RC electro-thermal model (SoC estimation using RC equivalent model and heat estimated through both reversible (entropy-based) and irreversible (Joule losses) heat generation models).

physics-guided design. Despite the diversity of physics-inspired networks, PINNs have gained the most traction due to their organized framework and improved training stability. In general PINNs, physics is incorporated solely through the loss function, where physical constraints guide learning without altering the network's structure. Despite the strengths of physics-based deep learning models, data-driven models are often considered as more accurate in predictive tasks. A key reason is their simpler loss function structure, which facilitates a more efficient and direct learning process compared to physics-based models that often involve complex physical constraints.

In light of these advantages, hybrid models that combine physics-based and data-driven components have recently gained significant attentions. These models aim to leverage the strengths of both models – retaining physical interpretability while benefiting from the predictive power and computational efficiency of data-driven learning. For example, Liu et al. (2024) decreased dependency on physics via training a model based on physics simulated data to mimic physical behavior, in which the result of this model is further processed within a data-driven model responsible for error correction. Although the high accuracy of physics‑data hybrid machine learning models, training processes of these models can be challenging, particularly due to the dual focus on both physical and data-driven components. This complexity often results in longer training times compared to traditional deep learning models. To address this issue, this study proposes a novel framework called physics-guided feature transfer (PgFT), explained in Section 4. Rather than relying on training a single, large, and complex hybrid model, the proposed framework suggests a selective physical feature extraction and sharing strategy. This approach is particularly useful in applications where there is a need to share essential representations from a complex model to multiple lightweight models, thereby significantly reducing training time and computational cost.

3. Real-Life Operation-based EV Battery Status and Dynamics

In general, EVs undergo three distinct operational phases during daily usage: (1) charging, (2) driving, and (3) parking. This study proposes a unified battery status modeling framework that accounts for these real-world operational phases. Most existing battery modeling approaches handle these phases independently, often neglecting the coupled thermal and electrical dynamics that arise across transitions. While recent studies have emphasized real-time battery state estimation, integrated modeling of SoC and heat generation across all operational conditions remain limited from the fact that the high dynamics interactions occurring while transitioning between one phase and the other are being neglected. This study addresses this gap by introducing a multi-physics-informed modeling approach that fuses mechanical, electrical, and thermal principles with real-world EV data. To better understand the embedded battery system dynamics across different operational phases, three scenarios capturing the real-life usage of the EV are proposed, as illustrated in <Figure 1>.

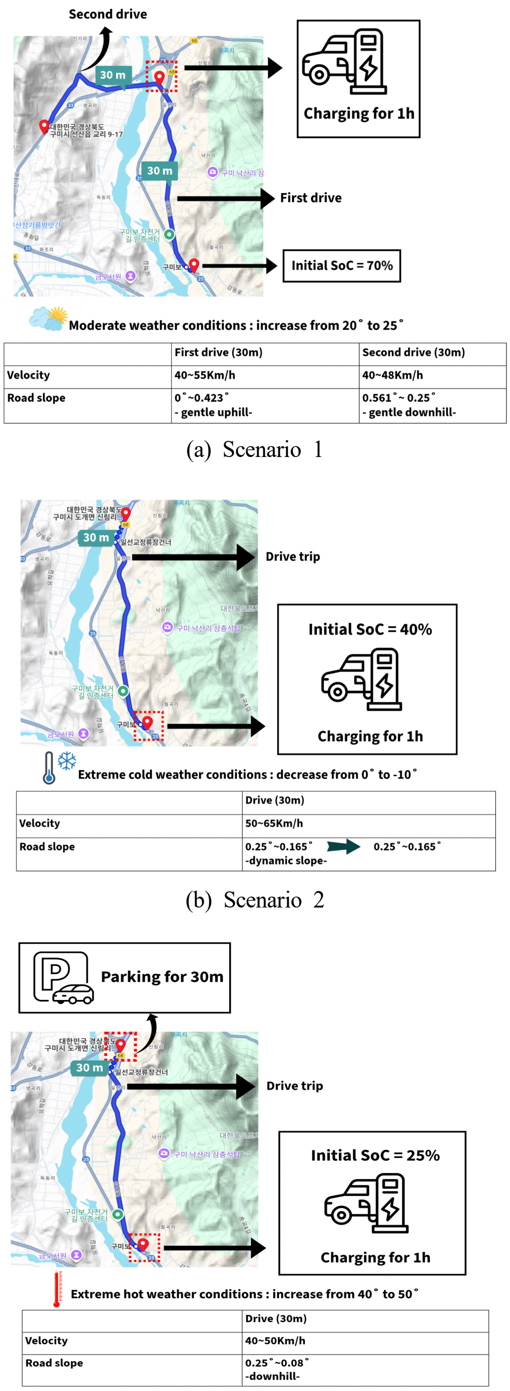

(a) Scenario 1

(b) Scenario 2

(c) Scenario 3

Figure 1. EV Operational Scenarios for Real-life Battery Performance Prediction

The dynamic characteristics of each scenario, including variations in driving velocity and road conditions, are depicted in <Figure 1>. In this study, a physics-based model is developed to characterize the dynamics of SoC and heat generation under various operational scenarios corresponding to the defined phases.

Scenario 1, where the EV undergoes an initial driving trip, is followed by a charging phase and a subsequent driving trip, as illustrated in <Figure 1(a)>. The total state of charge for this scenario is modeled using Equations (1) and (2):

$$SoC_{s1}(t) = 0.7 - \frac{C(t) - E(t)}{C_n} + \int_0^t \frac{I(t)}{C(t)} dt - \frac{C(t) - E(t)}{C_n} + N(t) \tag{1}$$

$$E(t) = \frac{P_{\infty}(t)}{V(t)},\ P_{\infty}(t) = \int_0^t \frac{P_{wheel}}{\eta_{(DC/AC)} \eta_{motor}} dt \tag{2}$$

$C(t)$ is the battery pack capacity, C_n is the nominal capacity. While $I(t)$ denotes the battery current, $V(t)$ is the battery voltage over time, and $N(t)$ is the associated noise term as will be explained later. The term $\eta_{(DC/AC)}$ represents the direct current (DC) to alternating current (AC) conversion efficiency, and η_{motor} is the motor efficiency. Accordingly, the wheel power (P_{wheel}) is a critical factor in the battery's energy modeling, since it represents the balance of the mechanical forces acting on the EV. As illustrated in <Figure 2>, the performance of an EV while driving is significantly influenced by the intricate dynamics of vehicle operation and resistive mechanical forces. These forces are: 1) rolling resistance (Fr) caused by wheel-road friction, 2) aerodynamic drag (Fa) represented by the air resistance, and 3) gradient resistance (Fg) resulting from slope dynamics and road conditions during driving cycles.

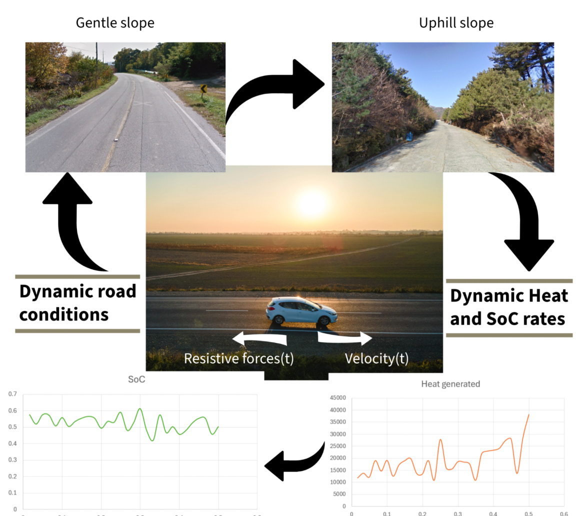

Figure 2. Influence of Driving Modes and External Conditions on the Battery Performance

Therefore, these external forces are considered in calculating the wheel power (P_{wheel}) as denoted by Equation (3).

$$P_{wheel} = v(t)(m \cdot d/dt v(t) + F_a(t) + F_r(t) + F_g(t) \quad (3)$$

$v(t)$ denotes the driving velocity, and m denotes the vehicle mass. The corresponding forces are defined in Equations (4 - 6).

$$F_a(t) = \frac{1}{2}\rho A C_d v(t)^2 \quad (4)$$

$$F_r(t) = m C_r a_g \cos(\alpha(t)) \quad (5)$$

$$F_g(t) = m a_g \sin(\alpha(t)) \quad (6)$$

While moving, the performance of an electric vehicle (EV) is influenced by the frontal surface area (A), drag coefficient (C_d), and rolling resistance coefficient (C_r). Further, air density (ρ), gravitational acceleration (a_g), and road gradient (α) significantly affect the overall driving efficiency and SoC of the EV. In the second scenario where the EV experience charging phase followed by a driving trip, the total SoC is modeled using Equation (7).

$$SoC_{s2}(t) = 0.4 + \int_0^t \frac{I(t)}{C(t)} dt - \frac{C(t) - Q(t)}{C_n} + N(t) \quad (7)$$

As mentioned earlier, most of the existing models particularly focus on the performance of EV battery systems during either charging or driving phases. However, in real-world EV operation scenarios, battery systems also experience charge losses during the parking phase due to the capacity fading phenomenon. Capacity fading is caused by self-discharge, which results from side electrochemical reactions occurring within the battery while it is at rest, in which the more degraded battery experiences a higher values of capacity fading. To address this phenomenon, the third scenario considers a realistic case where the EV undergoes charging, transitions to driving, and subsequently enters a parking phase. Accordingly, the relevant total SoC could be estimated using Equation (8).

$$SoC_{s3}(t) = 0.25 + SoC_{s2}(t) - \frac{C(t) - (C_{fade} + I_p)}{C_n} + N(t) \quad (8)$$

I_p is the charge loss while parking, and the capacity fade (C_{fade}) is denoted by Equation (9) where SoC_p represents the SoC during parking, T_p denotes the ambient temperature during the parking period, and t_p indicates the duration of parking.

$$C_{fade} = (\alpha_{SoC} \cdot SoC_p^{\beta_{SoC}}(t) + \delta_{SoC}) \cdot (\alpha_T \cdot T_p^{\beta_T} + \delta_T) \cdot t_p^{\gamma} \quad (9)$$

As this study considers real operational modes of an EV, these parameters are analyzed based on real-world conditions and their estimations: α_{SoC}=0.04, β_{SoC}=0.57, δ_{SoC}=0.26, α_T=4*10^{-9}, β_T=1.33, δ_T=3.00, and γ=4*10^{-2}, in alignment with the proposed scenarios. In addition, these values are adjusted in various testing environments.

EVs experience substantial thermal dynamics throughout their operations. The heat generation from various mechanical and electrochemical processes drives these dynamics. In this study, the heat generation behavior is modeled for each scenario, incorporating these thermal phenomena under realistic operating conditions. Specifically, for Scenario 1, the heat generation $Q_{s1}(t)$ is quantified using Equations (10).

$$Q_{s1}(t) = C_h(2P_m(t) + P_{ch}(t)) + 2H_{moving} + H_{charging} + N(t) \quad (10)$$

C_h is the battery heat coefficient. $P_m(t)$ and $P_{ch}(t)$ are the power consumed while driving and charging phases, respectively. H_{moving} and $H_{charging}$ denote the corresponding heat losses associated with vehicle driving and charging processes, respectively.

$$P_m(t) = \int_0^t V(t) \cdot I(t) dt + P_{co}(t) \quad (11)$$

$$P_{ch}(t) = SoC(0) \times C_n \times V_{nom} + \int_0^t V(t) \cdot I(t) dt \quad (12)$$

$SoC(0)$ is the initial SoC, V_{nom} is the nominal voltage of the battery pack.

$$H_{moving} = I(t)(OCV - V(t)) - I(t)\,T(t)\frac{\partial OCV}{\partial T} \quad (13)$$

Where OCV denotes the open-circuit voltage, representing the terminal voltage when the battery is under no-load conditions, and $T(t)$ is the temperature at at time t. The heat generated during the charging phase $H_{charging}$ is computed using the same thermal model applied in the moving phase, with distinct input values for charging current, voltage, OCV, and temperature reflecting the specific charging conditions.

$$H_{charging} = I(t)(OCV - V(t)) - I(t)\,T(t)\frac{\partial OCV}{\partial T} \quad (14)$$

Subsequently, the total heat generated in Scenario 2 is denoted by Equation (15).

$$Q_{s2}(t) = C_h(P_{ch}(t) + P_m(t)) + H_{charging} + H_{moving} + N(t) \quad (15)$$

In Scenario 3, which incorporates a parking phase, the total heat generated is modeled using Equation (16).

$$Q_{s3}(t) = C_h(P_{ch}(t) + P_m(t) + I_p) + H_{charging} + H_{moving} + H_{parking} + N(t) \tag{16}$$

In which,

$$N(t) = \Sigma_{i=0}^{Z_g} \Sigma_{j=0}^{Z_f} \lambda_{g,i} \cdot V_{g,i} \cdot N_g(0, C_{1,i}) + \lambda_{f,j} \cdot V_{f,j} \cdot N_f(0, C_{2,j}) \tag{17}$$

N_g follows Gaussian noise for general noise (genral inaccuracies), while N_f follows Gaussian noise for EV fluctuation noise (e.g., auxiliary power demands). The total number of noise sources considered in each operation phase is denoted by Z_g and Z_f for the general and fluctuation noise, respectively. The terms $\lambda_{g,i}$ and $\lambda_{f,j}$ are weighting factors that quantify the relative influence of general and fluctuation-based noise components, respectively. These weights are multiplied by the actual values ($V_{g,i}$ and $V_{f,j}$) of the corresponding noise sources. The terms $C_{1,i}$ and $C_{2,j}$ denote the variances associated with each noise component and are determined by comparing the outputs of the physical model with real-world EV operational data. In real-life EV applications, many disturbances such as sensor errors, measurement inaccuracies, and auxiliary components (e.g., pumps, HVAC systems) can be effectively modeled using Gaussian distributions. This is supported by the Central Limit Theorem, since these disturbances often result from the aggregation of numerous small, independent random factors, which collectively approximate a normal distribution. The following section outlines the detailed explanation of the proposed framework.

4. Dynamic Battery Performance Prediction using Physics-guided Feature Transfer Framework

As discussed in the previous section, the EV battery system is subject to various dynamic behaviors throughout different operational phases, influenced by multiple sources of noise and unexpected fluctuations. These complexities significantly impact the accuracy of predicting EVs' battery performances. An effective approach to tackling these challenges is through physics-based deep learning models, which can account for known physical dynamics. However, these models often suffer from several drawbacks, including longer training times, greater structural complexity, and higher computational costs as discussed in Section 2 and 3. These issues arise mainly due to the integration of physics-based energy functions into the learning process, which increases the burden during model training. Notably, such limitations are not exclusive to physics-based neural networks but are also prevalent in other large-scale or hybrid deep learning models.

To overcome these challenges, an effective method is to transfer the essential and informative features from a pretrained complex model to a simpler model, thereby enabling the latter to learn from distilled knowledge without inheriting the full computational load. In the context of physics-based models, a data-only model can serve as a more efficient alternative during both training and inference. However, as previously noted, purely data-driven models often fall short in capturing the dynamic uncertainties and environmental noise in EV battery systems. To address this challenge, this study proposes a physics-guided feature transfer (PgFT) framework as shown in <Figure 3>.

The core idea of this framework is to enable selective feature

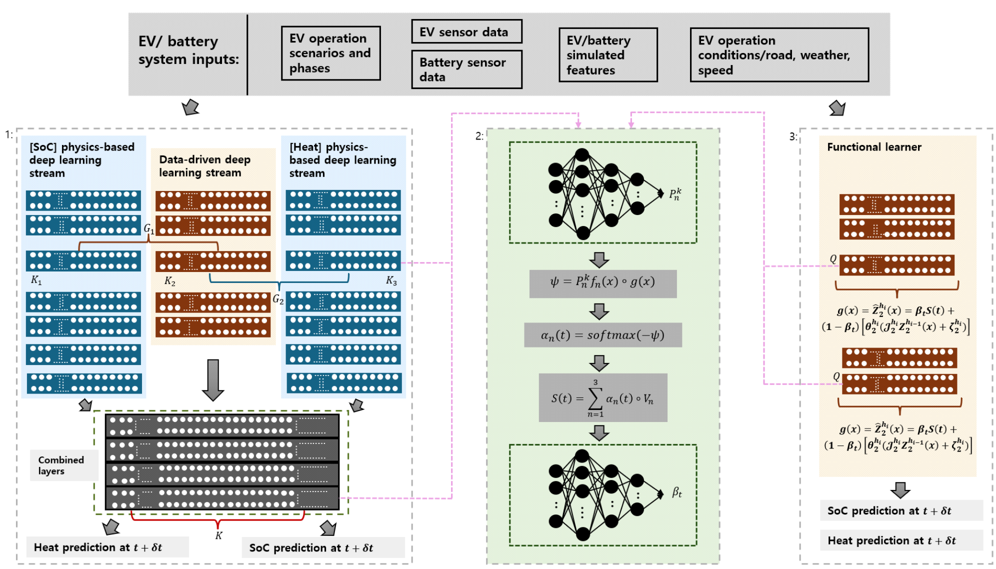

Figure 3. The Proposed PgFT Framework

transfer from a complex physics-data hybrid model to a lightweight, functional learner model through an attention-inspired mechanism. The framework architecture consists of two main models, a hybrid deep learning model with three distinct streams: a) A physics-based stream for SoC prediction, which incorporates known electrochemical principles, b) A data-driven stream responsible for predicting both SoC and heat generation using sensor data, and c) A physics-based stream for heat generation, grounded in established thermodynamic equations. The second is a lightweight model (Functional learner), which initially mirrors the architecture of the data-driven stream (SoC and heat prediction) but is not a pure deep learning model. Instead, it is trained using a function-based mechanism that enables selective feature extraction and sharing from the pretrained hybrid model. This function particularly shares the features capturing the physical behavior of the system to ensure accurate prediction under limited computational resources.

As illustrated in <Figure 3>, the hybrid model is responsible for predicting both SoC and heat generation, guided by the combination of sensor data and the physical principles described in the previous section.

The functional learner model, by contrast, is a single-stream data-based model. To enrich this learner with physics-informed knowledge, a transfer function is incorporated into its architecture. During training, this function enables the learner to selectively receive features from the hybrid model. Once the training process is complete, the transfer ceases, and the functional learner becomes an independent, physics-informed model capable of making accurate predictions with reduced time and computational cost.

Between the two models, an attention-inspired mechanism operates as a gating process. It compares the features generated by the hybrid model with those of the functional learner model, and then applies a SoftMax-based weighting scheme. In this process, features absent from the functional learner (primarily physics-based features) are assigned higher weights, ensuring their transfer. This mechanism is further enhanced with a deep learning module, which progressively refines and reduces the transferred features until the functional learner is sufficiently trained on the essential physics-based information.

The proposed feature-sharing and transfer strategy is executed in two stages to ensure effective and targeted knowledge transfer. In the first stage, features are extracted and shared from the hidden layers of the hybrid model, specifically the third hidden layer. In the second stage, features are shared from the combined layers, which integrate representations from all three streams and thus encapsulate rich, global information for accurate prediction. Specifically, the fourth combined layer is shared in this stage. For the first stage sharing, a grouping strategy is introduced to structure the interaction between the streams. Particularly, the three streams are grouped into two overlapping groups: 1) Group 1 (G1): Stream 1 (SoC physics-based) and Stream 2 (data-driven for SoC and heat), and 2) Group 2 (G2): Stream 2 and Stream 3 (heat physics-based). This grouping is motivated by the architectural overlap – Stream 2 is common to both the hybrid model and the target model. The features shared from both the hidden and combined layers represent the nonlinear transformations learned within the network. These transformations reflect the intricate dependencies embedded in the trained layers and are mathematically expressed as follows:

$$f_1(x) = \hat{Z}^{h_i}_{SoC}(x) = \theta^{h_i}_{SoC}(W^{h_i}_{SoC} Z^{h_{i-1}}_{SoC}(x) + b^{h_i}_{SoC}) \quad (18)$$

$$f_2(x) = \hat{Z}^{h_i}_{1}(x) = \theta^{h_i}_{1}(W^{h_i}_{1} Z^{h_{i-1}}_{1}(x) + b^{h_i}_{1}) \quad (19)$$

$$f_3(x) = \hat{Z}^{h_i}_{Heat}(x) = \theta^{h_i}_{Heat}(W^{h_i}_{Heat} Z^{h_{i-1}}_{Heat}(x) + b^{h_i}_{Heat}) \quad (20)$$

θ^{h_i} is the activation function for the hidden layer number i, W^{h_i} is the weight, and b^{h_i} is the bias. The notation SoC represents the SoC physics-based stream, 1 refers to the data-based stream in the hybrid model, and $Heat$ is the heat generated physics-based stream. In general, physics-informed models are designed to minimize an energy function that encapsulates the fundamental principles governing the physical system (Lee, 2023). Thus, for the SoC and heat generated streams, a physics-based energy function is developed for each scenario to effectively capture and predict the dynamics of each of them. Equations (21-26) defines the energy function for Scenario m ($m \in [1,2,3]$).

$$E^{m=1}_{SoC} = \frac{1}{N}\sum_{u=1}^{N} SoC_{s1}(t) - 2\left(\frac{-OCV \pm \sqrt[2]{(OCV)^2 - 4(-R)(-P_{mo}C_0)}}{2(-R)}\right)/c(t))^2 \quad (21)$$

R denotes the internal resistance of the battery, C_0 represents the coulombic efficiency, and P_{mo} refers to the power demanded by the EV motor.

$$E^{m=1}_{Heat} = \frac{1}{N}\sum_{u=1}^{N}(Q_{s1}(t) - 2(V(t)P_m(t)))^2 \quad (22)$$

$$E^{m=2}_{SoC} = \frac{1}{N}\sum_{u=1}^{N}(SoC_{s2}(t) - \left(\frac{-OCV \pm \sqrt[2]{(OCV)^2 - 4(-R)(-P_{mo}C_0)}}{2(-R)}\right)/c(t))^2 \quad (23)$$

$$E^{m=2}_{Heat} = \frac{1}{N}\sum_{u=1}^{N}(Q_{s2}(t) - (V(t)P_m(t)))^2 \quad (24)$$

$$E^{m=3}_{SoC} = \frac{1}{N}\sum_{u=1}^{N}(SoC_{s3}(t) - \left(\frac{(C_n - C_{fade})V_{nom}}{C(t)}\right)^2 \quad (25)$$

$$E_{Heat}^{m=3} = \frac{1}{N}\Sigma_{u=1}^{N}(Q_{s3}(t) - (V(t)C_{fade}))^2 \quad (26)$$

In which, N is the number of samples. Consequently, the total energy function for the combined streams is defined by Equation (27) for each scenario (m).

$$E = W_1(E_{SoC}^m + E_{Heat}^m) + W_2 E_{data} \quad (27)$$

W_1 and W_2 are the considered scaling factors for each energy function. E_{data} represents the data-driven energy function, as denoted by Equation (28).

$$E_{data} = \frac{1}{N}\Sigma_{u=1}^{N}(Y_o - Y_{true})^2 \quad (28)$$

Y_o denotes the predicted value of the SoC and heat generated, while Y_{true} represents the true value of them for each scenario. As a result, the functional learner is significantly simpler than the hybrid deep learning model. It has a lightweight architecture that relies on a limited set of informative features shared from the pre-trained hybrid deep learning model. Hence, it learns, and trains based on a defined function in its third and last layers structure denoted by Equation (29) where J^{h_i} and ζ^{h_i} are the coefficients for the hidden layers in the model, and β_t is a hyper-parameter decides the amount of feature shared at each time t.

$$g(x) = \hat{Z}_2^{h_i}(x) = \beta_t S(t) + (1-\beta_t)[\theta_2^{h_i}(J_2^{h_i} Z_2^{h_{i-1}}(x) + \zeta_2^{h_i})] \quad (29)$$

The shared features are incorporated into a function denoted as $S(t)$. $S(t)$ term is derived through a cross-attention-inspired mechanism between the three-stream hybrid model and the functional learner model. Specifically, the features to be shared from the three streams $f_n(x), n = 1,2,3$ serves as the keys K_n and the corresponding layer in the functional learner model $g(x)$ acts as the query Q Based on this, the first step of sharing starts with Equation (30).

$$\psi = P_n^k f_n(x) \circ g(x) \quad (30)$$

In general, the hidden structures of the streams in the hybrid model are more complex than those in the functional learner. Consequently, a direct element-wise (Hadamard) product between the corresponding hidden layers cannot be performed unless the dimensions of matrix resulted from the hidden layers are compatible. To address this issue, a projection matrix term P_n^k is introduced. This matrix is learned through a deep learning model that maps the features from each stream $f_n(x)$ in the hybrid model to the corresponding representation in the functional learner model $g(x)$. Once the dimensions are aligned using the projection, the element-wise product is applied. Then, the importance weight of each stream's features is computed using the following expression:

$$\alpha_n(t) = softmax(-\psi) \quad (31)$$

In conventional attention-based models, the SoftMax function emphasizes features with higher relevance scores, thereby assigning them greater weights. However, in this study, our objective is to prioritize and share the non-relevant features, which in our context correspond to the underlying physical features that may appear less dominant but carry essential information for accurate prediction. To achieve this, we incorporate a negative sign inside the SoftMax function, which reverses the attention distribution. This inversion allows the model to more easily identify features with lower relevance and assign them higher weights, ensuring that these subtle yet physically meaningful signals are effectively transferred to the learner model. Usually, in conventional attention-based approaches, the attention weight is typically multiplied by a corresponding value vector V_n, which corresponds to the features intended for sharing. In this study, the value term is defined as $V_n = f_n(x)$ corresponds to the feature representation from the n[th] stream of the hybrid model. Accordingly, the shared feature term $S(t)$, introduced earlier, is modeled as denoted by Equation (32).

$$S(t) = \Sigma_{n=1}^{3}\alpha_n(t) \circ V_n \quad (32)$$

Returning to Equation (29), which includes the parameter β_t, this parameter plays a critical role in controlling the level of dependency of the functional learner on the hybrid model. As time progresses, the functional learner is expected to learn from the shared features and gradually reduce its reliance on the hybrid model. This adaptive behavior is governed by the value of β_t, which decreases over time. To dynamically estimate β_t, a deep learning model is employed. The input to this model includes: 1) the current value of β_t, 2) the maximum attention weights max($\alpha_n(t)$) for each t, and 3) The difference between the outputs of the hybrid and the functional learner for both SoC and heat generation.

The deep learning model is trained to predict $\beta_{(t+\tau)}$, where τ represents the time increment. The objective of this model is to minimize $\beta_{(t+\tau)}$ toward zero over time, indicating a reduced reliance on the hybrid model as the functional learner becomes more self-sufficient and accurate in its predictions. To achieve this, the following energy function is designed using Equation (33).

$$E_{\beta} = \|\beta_{(t+\tau)} - \beta_t\| + \|\beta_{(t+\tau)} - \max(\alpha_n(t))\| \quad (33)$$

The first part of the energy function is to ensure that the update steps of $\beta_{(t+\tau)}$ remain smooth and gradual, preventing abrupt transitions in the sharing behavior. The second part is to encourage the value of $\beta_{(t+\tau)}$ to decrease progressively as the maximum attention weight max($\alpha_n(t)$) diminishes, reflecting a reduced dependency on the shared features from the hybrid model. In addition, a conditional mechanism is embedded in the model: once $\beta_{(t+\tau)}$ reaches zero, an "if" condition permanently assigns all future values of $\beta_{(t+\tau)}$ to zero. This condition ensures that, from that point onward, the functional learner operates independently, with no further feature sharing from the hybrid model. This framework is generalizable and can be applied to various scenarios where a pretrained deep learning model is required to share its essential features with a non-deep learning model, or even with multiple models.

In order to implement the proposed PgFT framework and obtain integrated data for predicting total SoC and heat generation, an EV combined dynamic simulator focusing on its battery system using CarMaker® (IPG Automotive, 2025) and Simscape® (MathWorks, 2025) along to PyBaMM® (PyBaMM, 2025) is developed and tested. Further, to demonstrate the effectiveness of the proposed framework, it is compared and analyzed against four other feature sharing frameworks. The proposed four comparison models share a similar structure with the proposed model (for both the hybrid model and the functional learner). However, each adopts a different sharing approach. In Comparison model 1, instead of the proposed two-stage grouping strategy, only the third-layer features are shared, with all streams grouped into a single group. While this design provides a simplified structure, it ignores earlier interactions between physics-based and data-driven features, causing the loss of important temporal and electrochemical correlations and reducing generalizability

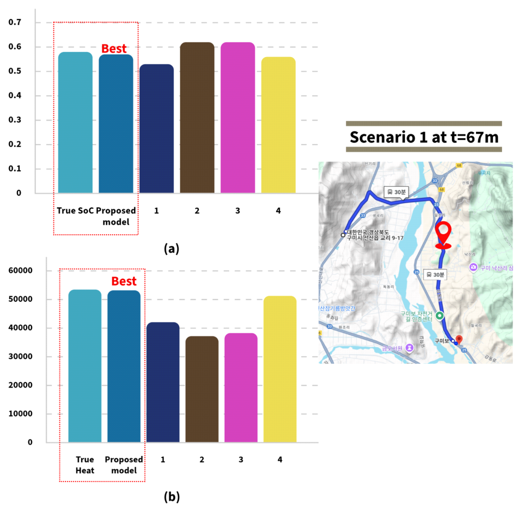

(a) Scenario 1

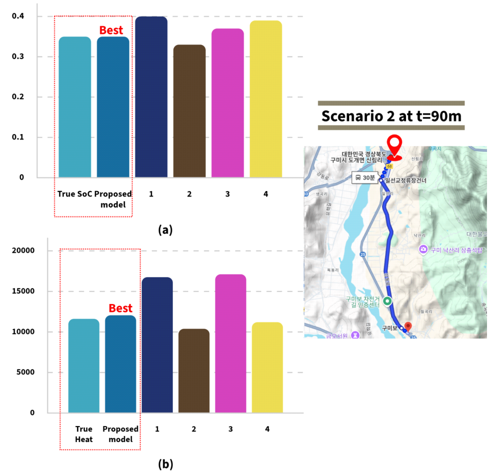

(b) Scenario 2

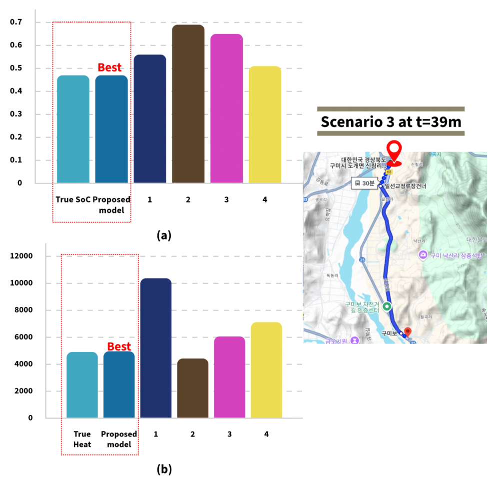

(c) Scenario 3

Figure 4. Comparative Analyses using the Proposed Framework and Comparison Models at Different Operation Durations

in realistic driving or charging conditions. Comparison model 2 follows a similar design, but the shared features are taken from the last layer of each stream instead of the third. Although the last layer contains higher-level representations, late sharing fails to capture intermediate interactions, resulting in weaker adaptability under dynamic conditions. In Comparison model 3, no sharing mechanism is applied; instead, the features from the last combined layer of the hybrid model are directly copied to the functional learner. This model provides the simplest structure and the shortest transfer time, however, it ignores the benefits of joint representation learning, leading to poor performance in scenarios with strong coupling between SoC and thermal dynamics. Comparison model 4 shares features from only 50% of each stream. Specifically, the fourth layer of the SoC and heat streams, and the third layer of the data-driven stream, are shared with the functional learner. While this model offers partial sharing to reduce overfitting, it results in unbalanced representation transfer, which causes instability when applied to realistic conditions where SoC and heat dynamics must be jointly modeled.

Both the proposed model and all comparison models were trained for 3000 epochs using a learning rate of 0.01 for the hybrid deep learning architecture. Across all models, the number of layers was kept consistent: seven layers were used for the SoC and heat streams, five layers for the data-driven stream. The predicted accumulated SoC and heat generation for the functional learner model, after applying the respective sharing strategy and completing the training process, were tested using the PgFT framework. All models were implemented in Python 3.12.11 (GCC 11.4.0) with the PyTorch library, trained for 3000 epochs using the Adam optimizer. The results were compared against both the ground truth values and the outcomes of the four comparison models. <Figure 4> demonstrates the accuracy

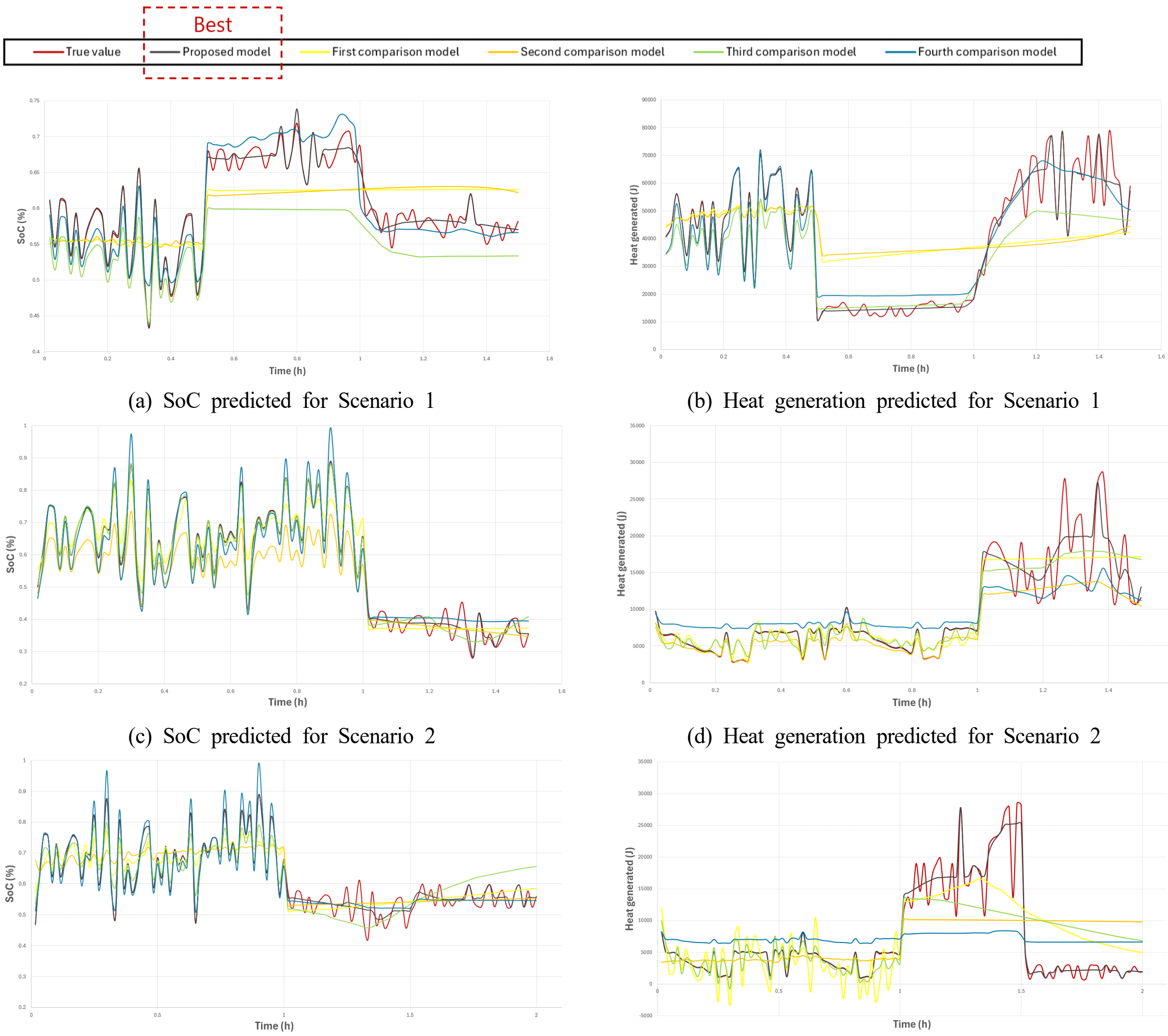

(a) SoC predicted for Scenario 1

(b) Heat generation predicted for Scenario 1

(c) SoC predicted for Scenario 2

(d) Heat generation predicted for Scenario 2

(e) SoC predicted for Scenario 3

(f) Heat generation predicted for Scenario 3

Figure 5. Predicted Total SoC and Heat Generation Across all Scenarios

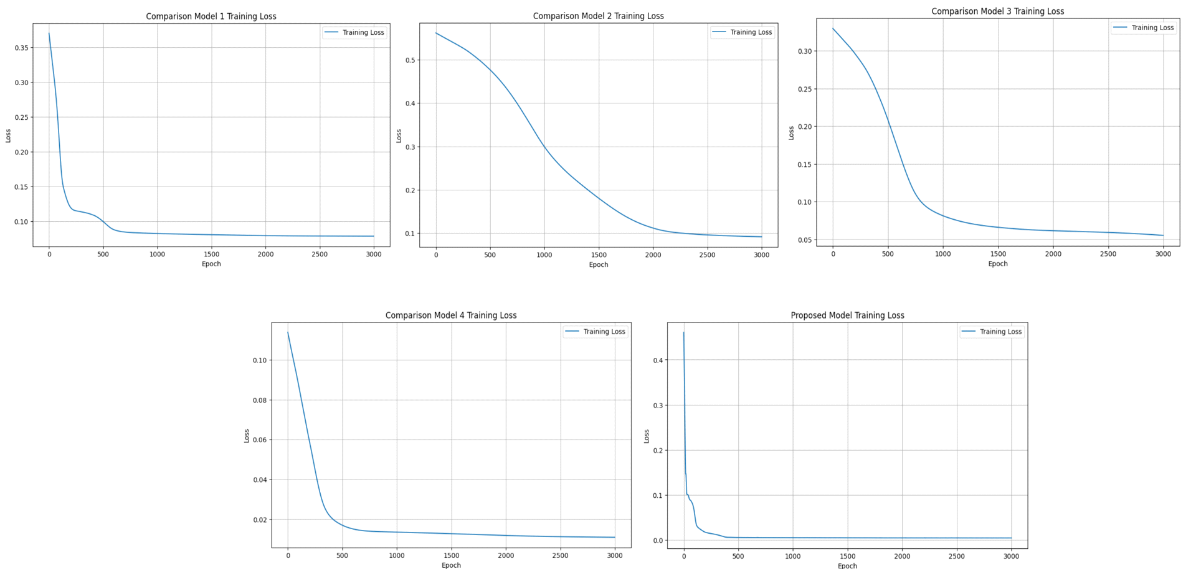

Figure 6. Training Loss Convergence of the Proposed and Comparison Models

Table 2. RMSE and MAE of the Proposed and Comparison Models

Model	RMSE	MAE
Proposed Model	0.013	0.009
Comparisom Model 1	0.047	0.040
Comparisom Model 2	0.053	0.048
Comparisom Model 3	0.046	0.041
Comparisom Model 4	0.015	0.011

and reliability of capturing the intricate dynamics of SoC and heat generation at different test durations during the operation of each scenario.

As shown in <Figure 4>, the proposed framework achieved the highest accuracy across all selected test durations in the evaluated scenarios. Despite the high dynamics and noise, the proposed framework effectively shared the meaningful features to capture unexpected nonlinearities within the system. The effectiveness of the proposed framework was further evaluated over the full duration of each scenario. <Figure 5> presents the predicted total SoC and total heat generation for each scenario.

As illustrated in <Figure 4> and <Figure 5>, the proposed PgFT framework consistently outperformed all comparison models. It effectively transferred the highly dynamic and unexpected behaviors of the system, which the alternative models failed to replicate across various operational points. These results clearly highlight the superiority and robustness of the proposed PgFT framework compared to the other approaches.

Furthermore, the training efficiency and convergence speed of the proposed model and the comparison models were evaluated based on the loss curves presented in <Figure 6>. The results indicate that the proposed model successfully facilitated the transfer of essential features while achieving faster convergence relative to the alternative feature-sharing strategies employed in the comparison models, which exhibited prolonged training times. Notably, Comparison model 2 demonstrated the slowest convergence, underscoring its relative inefficiency in terms of learning performance.

The root mean square error (RMSE) and mean absolute error (MAE) were computed for all comparison models to assess their estimation accuracy. These metrics were used to validate the predictive feasibility of each model, as summarized in <Table 2>.

As shown in <Table 2>, the proposed framework achieved the lowest values of the RMSE and MAE, demonstrating its superior accuracy in transferring the desired features and effectively guiding the model training process.

5. Conclusion

In this study, the EV battery performance are predicted using the proposed PgFT framework. The proposed PgFT framework integrates two stage cross attention-inspired sharing strategy to train a functional learner model to accurately predict total SoC and heat generation. This framework can be extended to other complex deep learning architectures, enabling the selective and limited transfer of pretrained features to simpler models across a wide range of applications.

References

Apostolakis, T. and Ampountolas, K. (2024), Physics-Inspired Neural Networks for Parameter Learning of Adaptive Cruise Control Systems, *IEEE Transactions on Vehicular Technology*, **73**(10), 14291-14301.

Ceraolo, M., Fioriti, D., Lutzemberger, G., Quilici, F. G., Scarpelli, C., and Bianchi, F. (2024), Electro-Thermal Modeling and Aging Evaluation of Lithium Battery Packs for Electric Vehicles, *IEEE Access*, **12**, 128151-128165.

Chen, Y., Kwak, K. H., Kim, J., Jung, D. D., and Kim, Y. (2024), Integrated Thermal Management of Electric Vehicles Based on Model Predictive Control with Approximated Value Function, *IEEE Access*, **12**, 58898-58914.

Chianese, G., Iannucci, L., Veneri, O., and Capasso, C. (2025), Real-Time Estimation of Battery SoC through Neural Networks Trained with Model-Based Datasets: Experimental Implementation and Performance Comparison, *Applied Energy*, **389**, 125783.

Guo, N. Z., Shi, K. Z., Li, B., Qi, L. W., Wu, H. H., Zhang, Z. L., and Xu, J. Z. (2022), A Physics-Inspired Neural Network Model for Short-Term Wind Power Prediction Considering Wake Effects, *Energy*, **261**, 125208.

IPG Automotive (2025), CarMaker, https://ipg-automotive.com/products-services/simulation-software/carmaker/.

Kim, J., Oh, J., and Lee, H. (2019), Review on Battery Thermal Management System for Electric Vehicles, *Applied Thermal Engineering*, **149**, 192-212.

Kumar, R. R., Bharatiraja, C., Udhayakumar, K., Devakirubakaran, S., Sekar, K. S., and Mihet-Popa, L. (2023), Advances in Batteries, Battery Modeling, Battery Management System, Battery Thermal Management, SoC, SoH, and Charge/Discharge Characteristics in EV Applications, *IEEE Access*, **11**, 105761-105809.

Lee, H. (2023), Physics-Based Cooperative Robotic Digital Twin Framework for Contactless Delivery Motion Planning, *International Journal of Advanced Manufacturing Technology*, **128**, 1255-1270.

Li, Y., Li, K., Liu, X., Li, X., Zhang, L., Rente, B., Sun, T., and Grattan, K. T. V. (2022), A Hybrid Machine Learning Framework for Joint SoC and SoH Estimation of Lithium-Ion Batteries Assisted with Fiber Sensor Measurements, *Applied Energy*, **325**, 119787.

Liu, Y., Wang, R., Gu, Y., Li, C., and Wang, G. (2024), Physics-Inspired and Data-Driven Two-Stage Deep Learning Approach for Wind Field Reconstruction with Experimental Validation, *Energy*, **298**, 131230.

Maheshwari, A. and Nageswari, S. (2022), Real-Time State of Charge Estimation for Electric Vehicle Power Batteries Using Optimized Filter, *Energy*, **254**(B), 124328.

MathWorks (2025), Simscape, https://www.mathworks.com/products/simulink.html.

Mesbahi, T., Sugrañes, R. B., Bakri, R., and Bartholomeüs, P. (2021), Coupled Electro-Thermal Modeling of Lithium-Ion Batteries for Electric Vehicle Application, *Journal of Energy Storage*, **35**, 102260.

Pang, H., Wu, L., Liu, J., Liu, X., and Liu, K. (2023), Physics-Informed Neural Network Approach for Heat Generation Rate Estimation of Lithium-Ion Battery under Various Driving Conditions, *Journal of Energy Chemistry*, **78**, 1-12.

PyBaMM (2025), Python Battery Mathematical Modelling. https://pybamm.org.

Seyed-Ahmadi, A. and Wachs, A. (2022), Physics-Inspired Architecture for Neural Network Modeling of Forces and Torques in Particle-Laden Flows, *Computers & Fluids*, **238**, 105379.

Wang, J., Lv, J., Lin, W., Song, W., and Feng, Z. (2024), Heat Generation Rate Estimation of Lithium-Ion Batteries for Electric Vehicles by BP-Based Optimized Neural Network, *Applied Thermal Engineering*, **253**, 123752.

Wu, Y., Huang, Z., Li, D., Li, H., Peng, J., Stroe, D., and Song, Z. (2024), Optimal Battery Thermal Management for Electric Vehicles with Battery Degradation Minimization, *Applied Energy*, **353**, 122090.

Yalçın, S., Panchal, S., and Herdem, M. S. (2022), A CNN-ABC Model for Estimation and Optimization of Heat Generation Rate and Voltage Distributions of Lithium-Ion Batteries for Electric Vehicles, *International Journal of Heat and Mass Transfer*, **199**, 123486.

Zahid, T., Xu, K., Li, W., Li, C., and Li, H. (2018), State of Charge Estimation for Electric Vehicle Power Battery Using Advanced Machine Learning Algorithm under Diversified Drive Cycles, *Energy*, **162**, 871-882.

Author Profile

Raghda Mansour Kamel Noureldin: She received her bachelor's degree in Industrial Engineering from the University of Jordan in 2021 and her master's degree in Industrial Engineering from Kumoh National Institute of Technology in 2025. She is currently working as a researcher in the energy field at the Research Center of Energy Convergence Technology, Pusan National University. Her research interests include electric vehicle battery systems, physics-based modeling, and deep learning.

Hyunsoo Lee: Ph.D. degree in Industrial and Systems Engineering Department at Texas A&M University, College Station, TX, USA in 2010. He received the M.S. degree in Industrial Engineering from POSTECH, Korea in 2002. He is a Professor in School of Industrial Engineering at Kumoh National Institute of Technology, Korea from 2011. His research interests include nonlinear optimization and control, quantum computing, deep learning, and smart manufacturing.